

Synthesis of single-walled carbon nanotubes by dual laser vaporization

M.K Moodley^{a,b*}, N.J Coville^c, B.C Holloway^d and M. Maaza^e

Single-walled carbon nanotubes were synthesized by the laser vaporization of graphite composite targets in a tube furnace. Two pulsed Nd:YAG lasers operating at fundamental (1064 nm) and 2nd harmonic (532 nm) frequencies were combined, focussed and evaporated targets in an inert argon atmosphere at a pressure of 500 mbar. Furnace temperatures of either 1200 or 1000°C were used. The targets were either pure graphite or graphite doped with catalysts. The as-evaporated material was collected and characterized by transmission electron microscopy, scanning electron microscopy and Raman spectroscopy. TEM analysis showed individual single-walled tubes with diameters of 1.31 ± 0.02 nm and bundles of single-walled tubes up to 10 nm in diameter. Raman spectroscopy revealed a distribution of chiral, metallic and semiconducting nanotubes, all with a very low defect concentration. Most of the identified tubes were semiconducting. The addition of Fe as catalyst changed the diameter distribution fractionally from 1.30–1.46 nm to 1.33–1.49 nm and significantly lowered the defect concentration. The concentration of metallic nanotubes was also found to have decreased.

Introduction

Bacon¹ first observed tubular structures of carbon in 1950. In the 1970s, Endo² observed carbon nanostructures by transmission electron microscopy. However, it was only after a report by

^aNanoScience Research Group, Material Science and Manufacturing, CSIR, P.O. Box 395, Pretoria 0001, South Africa.

^bSchool of Physics, University of the Witwatersrand, Private Bag 3, WITS 2050, South Africa.

^cSchool of Chemistry, University of the Witwatersrand.

^dDepartment of Applied Science, College of William & Mary, 328 McGlothlin-Street Hall, Williamsburg, VA 23187-8795, U.S.A.

^eThemba LABS, P.O. Box 722, Somerset West 7129, South Africa.

*Author for correspondence. E-mail: mkmoodley@csir.co.za

Iijima³ in 1991 that there was a surge in the scientific interest in this type of carbon material. Indeed, it can be said that carbon nanotubes gave birth to what we now know as nanoScience and nanotechnology. The scientific interest in this material is based on the unique electrical,⁴ chemical,⁵ optical⁶ and mechanical⁷ properties associated with nanotubes. Applications of nanotubes to make devices have already been extensively reported in the scientific literature.⁸⁻¹¹ Whilst many device applications have been demonstrated, a major obstacle is the reliable synthesis of carbon nanotubes. The problem arises because carbon nanotubes form by the self-assembly of atoms in the vapour phase. Depending on the experimental conditions under which self-assembly takes place, the characteristic properties of nanotubes such as chirality, length and diameters will vary in the final product. While various investigations¹² were conducted on the influence of experimental conditions on the laser synthesis of single-walled carbon nanotubes (SWCNTs), to date, no experimental technique or recipe has been developed to pre-determine or successfully reproduce a specific type of carbon nanotube, in particular in regard to its chirality.¹³ This article reports on the method of dual laser vaporization to synthesize carbon nanotubes, in particular the synthesis of single-walled nanotubes and our attempt to achieve control of their diameter, which in turn affects the electronic properties.

Growth mechanisms

Uncapped single-walled carbon nanotubes can be visualized as a two-dimensional graphene sheet, rolled-up to form a seamless tube. The manner in which the tube is rolled determines whether it will be metallic in nature or semiconducting. Typically, SWCNTs have diameters in the order of a few nanometres with lengths of up to a few hundred micrometres. Overviews on carbon nanotubes, including a mathematical description of their structures, can be found in several texts.^{8,9,14}

A common feature of all experimental methods used in the synthesis of carbon nanotubes is having carbon atoms in the vapour form prior to self-assembly. In the case of SWCNTs, a further prerequisite is to use transition metal catalysts, for example Fe, Ni and Co.^{15,16} Otherwise, the atoms self-assemble to form multi-walled carbon nanotubes (MWCNT) or, if self-assembly is absent, 'nanosoot' forms of carbon. The self-assembly process at the multi-atomic level to create specific CNTs is not fully understood. This means that controlled large-scale synthesis is not yet possible. Numerous research groups have proposed theories based on experimental observa-

tions and computational modelling.¹⁷ However, each has its advantages and disadvantages. This suggests that there could be more than one mechanism involved in the self-assembly process. These accounts can be found elsewhere.^{8,9}

Dual laser synthesis of SWCNTs

The use of a pulsed infrared laser to synthesize fullerenes and later tubular fullerenes was originally investigated by Smalley's research group.^{15,16} The laser was chosen as the power source as the energy directed on the target in a very short time, in the order of nanoseconds, is very intense. This was sufficient to create a plasma of carbon vapour in the vicinity of the irradiated target. The temperature of the plasma is in the region of 10 000°C. As the plasma plume expands, it cools down. It is at this stage that the carbon atoms coalesce to form nanotubes. Another important aspect of using lasers is the repeatability and control of laser parameters, which ensures that the experimental conditions are kept constant for reliable synthesis of nanotubes. In Smalley's work,^{15,16} a graphite target doped with a few per cent of transition metals yielded SWCNTs in the product. The addition of a second laser, made co-linear with the first, raised the yield of the tubes. The use of two lasers increased the concentration of vaporized carbon atoms in the plasma plume.¹⁸ This was achieved by delaying the arrival of the pulsed Nd:YAG laser light at 1064 nm at the target by a few tens of nanoseconds with respect to the first laser pulse at 532 nm, which is primarily responsible for vaporizing sub-micrometre layers of the composite target. At this instant, plasma is generated very near to the target surface. The plasma shields the target from the second pulse. The interaction of the latter with the plasma plume creates reverse Bremsstrahlung, that is, the charged particles within the initial plasma absorb laser photons of the second pulse. In the process, the plasma intensity increases rapidly, creating more ionized carbon atoms that subsequently coalesce.

Experimental details

Figure 1 is a schematic illustration of the experimental set-up to synthesize SWCNTs. It is similar to that used at Rice University¹⁶ and elsewhere.^{19,20} Two pulsed Nd:YAG beams are made co-linear, combined and directed towards a graphite composite target located in a tube furnace. The one was a Continuum Surelite SL-10 operating at $\lambda = 532$ nm with a maximum energy of 70 mJ per pulse; the second laser was a Spectra Physics GCR 130 operating at $\lambda = 1064$ nm and energy of 330 mJ per pulse. Both operated at a 10-Hz repetition rate and with pulse widths between 8–12 ns. Both lasers were focussed to a diameter of approximately 3 mm on the target. The 1064-nm laser had a fluence at the target of 4.6 J cm^{-2} ; that of the other laser was 1 J cm^{-2} , because of its limited available energy of the latter. To prevent pitting of the target by focusing the 532-nm laser beam any further and thereby increasing particulate formation, the trade-off was to operate it with a smaller beam intensity. The target was raster scanned for uniform evaporation.

Target preparation and operation

The targets were pressed from a paste containing ultra-fine 99.9% graphite powder, transition metal nitrates and Dylon®. The targets were vacuum baked for 4 hours and then out-gassed in an inert environment for several hours at operating temperatures before the start of the experiments, to remove volatiles. Table 1 shows the composition of targets used in the experiments. The 25-mm-diameter targets were located at the centre of a vacuum-sealed, 60-mm-diameter, 1500-mm-long quartz tube.

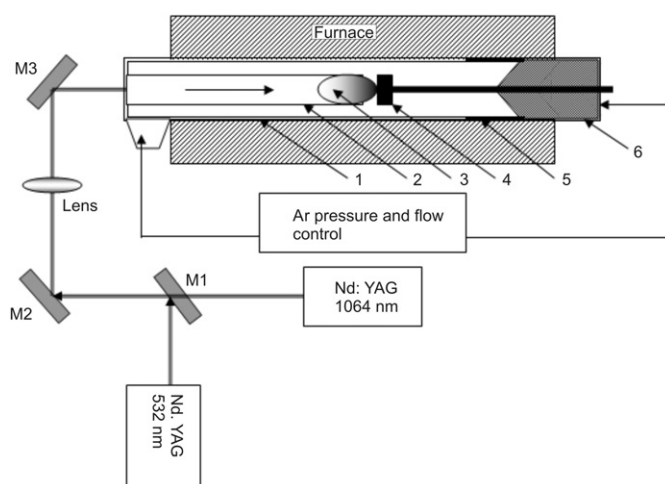


Fig. 1. A schematic illustration of the laser vaporization experimental set-up to synthesize SWCNTs. Beams from two pulsed lasers, operating at fundamental and first harmonic frequencies, respectively, were combined by mirrors M1–M2. The beams enter a sealed quartz tube (1). The flow and pressure of argon gas is electronically controlled by MKS instrumentation. The gas flow is confined to the inner quartz tube (2) before it reaches a graphite composite target (4) located centrally in a high-temperature furnace. A carbon plasma plume (3) is generated when the M3 mirror raster scans the target (4). The vaporized target material condenses at the rear (5) of the furnace, where it is cooled by a water-cooled copper collector (6).

The target was screwed onto a stainless steel push rod, which extended out of the furnace, for easy placement in the furnace. The front end of the quartz tube was fitted with an anti-reflection coated laser window and inlet gas connections. A second quartz tube, 19 mm in diameter, was fitted concentrically within the larger quartz tube. The smaller tube extended from the entrance window to just before the target. The tube provided a laminar flow of argon gas towards the target in the same direction of the laser beams. The argon acted as a buffer by slowing the outwardly expanding carbon plasma plume. This slowing down of the plume facilitates self-assembly of the carbon atoms into SWCNTs.¹⁹ The gas also carries the nanotubes towards the back of the furnace. A water-cooled copper collector was fitted at the rear of the quartz tube for sample collection. During operation, a constant flow of Ar gas at $200 \text{ cm}^3 \text{ min}^{-1}$, at a pressure of 500 mbar was maintained by a MKS flow and pressure controller. The target was out-gassed at operating temperatures. Initial experiments were conducted at 1200°C (target T2) and the remainder of the experiments (targets T1, T3 and T4) were carried out at 1000°C for we considered that at 1200°C the defect concentration would be high in the synthesized material. Each target was evaporated for between 4 and 5 hours. The as-evaporated material that was deposited in the relatively cool surfaces at the end of the quartz tube, was collected and characterized by transition electron microscopy (TEM), scanning electron microscopy (SEM) and Raman spectroscopy (RS).

Table 1. Target composition.

Target reference	Composition (%)	Temperature (°C)
T1	C (100)	1000
T2	C (98.8): Ni (0.6): Co (0.6)	1200
T3	C (98): Ni (1): Co (1)	1000
T4	C (98): Fe (0.67): Ni (0.67): Co (0.67)	1000

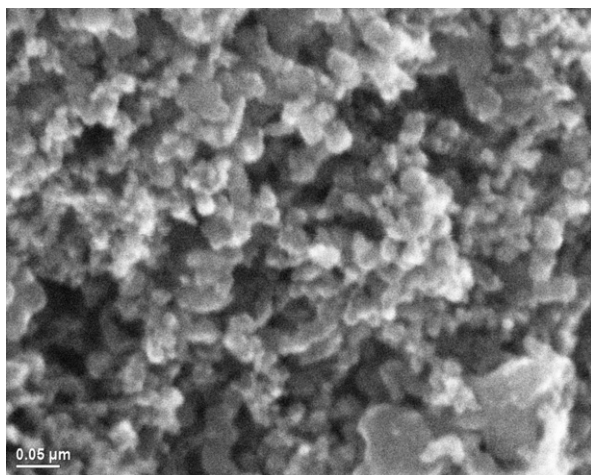


Fig. 2. SEM image of as-evaporated material from catalyst-free target T1. Only spherical carbon 'nanosoot' is evident, indicating the importance of catalysts if nanotubes are to be synthesized.

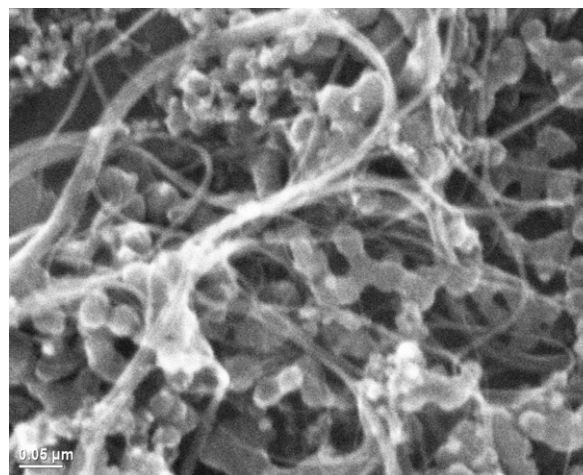


Fig. 3. SEM image of as-evaporated material from target T3, showing a combination of soot, bundles and individual nanotubes. Bundles dominate because of the strong van der Waals forces between the tubular walls of SWCNTs.

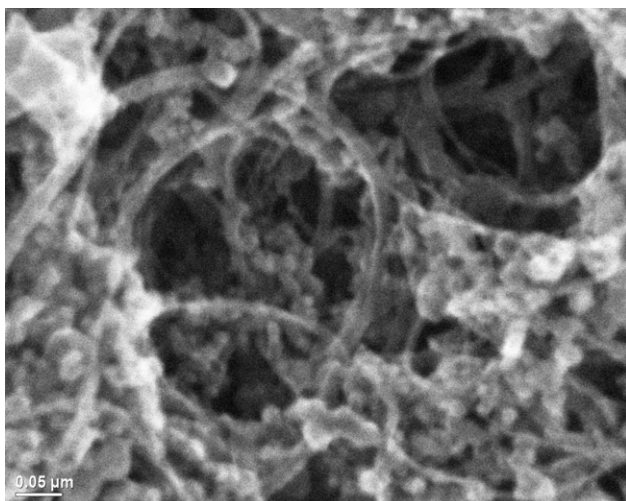


Fig. 4. SEM image of material obtained from target T4, resembling that in Fig. 3.

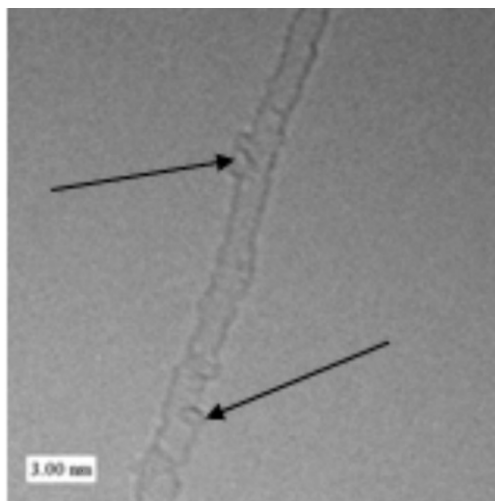


Fig. 5. TEM image of an individual SWCNT obtained by vaporising target T2. The arrows point to defects along the tube walls. Tube diameter is 1.3 nm. Scale bar: 3 nm.

Results and discussion

Figure 2 is an SEM image of material evaporated from a catalyst-free target. Nanospheres of carbon soot are abundant in the image and there is no evidence of SWCNTs. SEM images of as-evaporated samples from targets T3 (Fig. 3) and T4 (Fig. 4) show individual and bundles of SWCNTs. The product resembles 'spaghetti'. Dispersed with the bundles are nanospheres of carbon soot. The diameter of these particles was in the range 10–25 nm.

Figure 5 shows a TEM image of an isolated SWCNT of diameter 1.3 nm, synthesized from target T2. Structural defects are visible along the tube length, indicating malformation during self-assembly of carbon atoms. Figure 6 shows another TEM image of as-evaporated material from T2. Here, a bundle of SWCNTs clumped together by van der Waals forces can be seen. As in Fig. 7, most TEM images showed SWCNTs appearing as bundles up to 10 nm in diameter. The darker spots are the transition metal catalysts. Close observation shows that the nanotubes appear to nucleate at these sites. The maximum size of the nanotube bundles appears to be close to the diameter of the catalyst particles. Further investigation by means high-resolution TEM is needed to investigate the metal catalyst–nanotube bundle interface.

Raman spectroscopy has become the most widely used technique to characterize CNTs because of its ability to provide

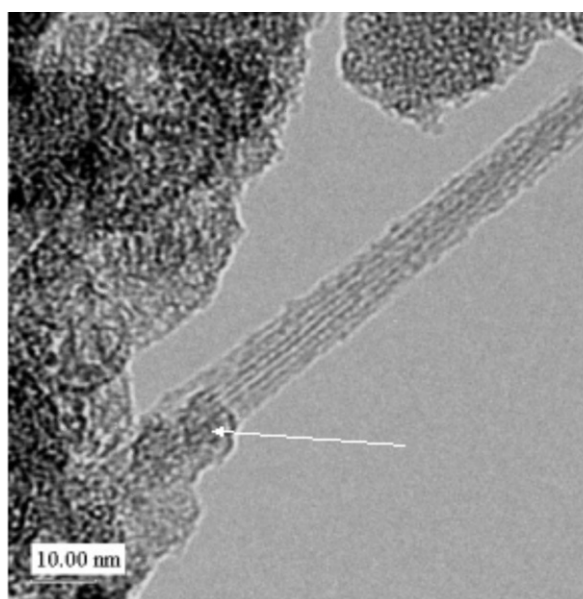


Fig. 6. TEM image of as-evaporated material showing 6 or 7 SWCNTs bundled together. The arrow points to the region of initial nucleation. These sites are metallic catalysts, which are important in the formation of single-walled tubes.

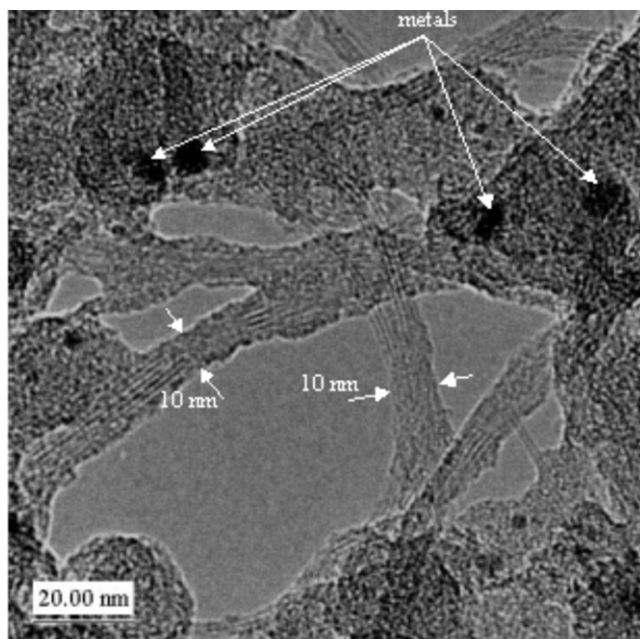


Fig. 7. TEM image of as-evaporated material from target T3. The arrows indicate bundles of SWCNTs up to 10 nm in diameter. The darker regions are metal catalysts.

information on electronic and structural properties. The three most important spectral features of Raman spectra of SWCNTs are:⁸ (a) the radial breathing mode frequency, ω_{RBM} , in the region of 100–300 cm^{-1} ; (b) the disordered D-band around 1350 cm^{-1} ; and (c) the G-band in-plane bond stretching modes between 1500–1600 cm^{-1} .

An empirically determined, approximate relationship between ω_{RBM} and the SWCNT diameter (in nm) is given by the formula^{21,22}

$$d = \frac{223.5}{\omega_{\text{RBM}} - 12.5 \text{ cm}^{-1}}$$

The relatively quick time to record a Raman spectrum (5 minutes) at a laser focus spot means that a statistical analysis of a large sample area can be performed to determine the homogeneity of the material. This is particularly useful for determining the distribution of CNTs according to chirality, diameter, defects, and class types. For the Raman measurements, a slightly defocused $\lambda = 514.5 \text{ nm}$ laser beam (green) was directed onto the sample, which was placed on a microscope glass slide. The laser power at the focal spot was 1.25 mW. Defocusing avoided localized burning or heating of the sample. Raman analysis of material obtained from T1 showed no spectral features and was ignored. Such a spectrum indicates that the material was amorphous, since no phonon resonance, typical of an ordered bounded structure, was detected. Figure 8 shows a Raman spectrum of T3 material taken at two different spots. This is a typical spectrum of individual and bundles of SWCNTs. The three main regions of the spectrum can be clearly identified.

Using Equation (1), analysis of ω_{RBM} modes at around 183 cm^{-1} indicated tube diameters of $1.31 \pm 0.02 \text{ nm}$. The D-band situated at 1350 cm^{-1} is representative of defects within sp^2 hybridized C–C bonds. A broad and low-intensity peak indicates a small concentration of defects within the tubular structures. At the G-band between 1500 and 1600 cm^{-1} , two spectral features stand out, the lower G frequency (G^-) and upper G frequency (G^+). The relative shape and intensity difference between the G^- and G^+ peaks depend on whether the tubes are metallic or semiconducting. The strong intensities at 1561 and 1585 cm^{-1} , which can be fitted by Lorentzian distribution, indicate the presence of semi-

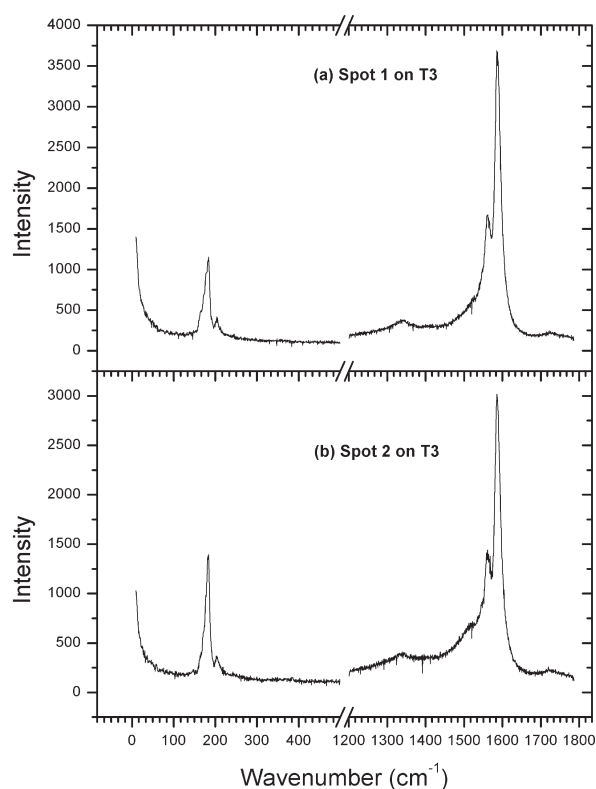


Fig. 8. Raman spectra corresponding to two different spots on target T3. The left-hand spectrum is a signature for SWCNTs. It reflects the radial breathing mode (RBM), where the tubes flex about their central axis and strongly correlates with their diameter. The width of this peak indicates the distribution of diameters of single-walled tubes. The right-hand spectrum describes the tangential features of the tube including whether it is metallic or semiconducting in nature.

conducting SWCNTs.²³ A slight broadening on the shoulder of the G^- peak at approximately 1511 cm^{-1} is evident at both sample spots. The line shape in this region is asymmetrical and typical of metallic tubes. Comparing the relative line intensities of the two regions of interest in the G band, identified above, we conclude that most of the sample material consisted of semiconducting nanotubes.

Figures 9a and 9b are Raman spectra showing the effect of a three-catalyst target (T4) compared with a two-catalyst combination (T3) on the production of nanotubes. It is clear from the spectra for T4 (Fig. 9a) that there is a larger distribution of larger diameter, and higher concentration, of SWCNTs than in the spectra of T3 as seen on the top trace (triangles) of the plot at peak positions (a)–(d), where the diameters vary from 1.33–1.49 nm, whereas for T3 this variation was from 1.31–1.46 nm. Second, the spectra for T4 (Fig. 9b), bottom trace (triangles) showed a lower intensity peak in regions (e)–(h). This implies: (a) a significant decrease in the defect concentration at the D-band (e); (b) a drop in the concentration of metallic tubes as shown in region (f); and (c) a higher concentration of semiconducting nanotubes as shown in the G^- and G^+ regions. These observations mean that the addition of Fe as a catalyst changed the SWCNTs' diameter distribution, reduced their defect concentration and also promoted the self-assembly of semiconductor nanotubes over metallic nanotubes. These results are similar, but not identical, to those of other researchers^{24,25} as the concentration of the Fe with respect to Co and Ni was different from those reported in refs 24 and 25. In the work of Lebedkin *et al.*,²⁴ the third catalyst was in the form of FeS and the atmosphere was a combination of hydrogen and argon. In their work, diameters up to 5.6 nm were observed. These relatively large diameters

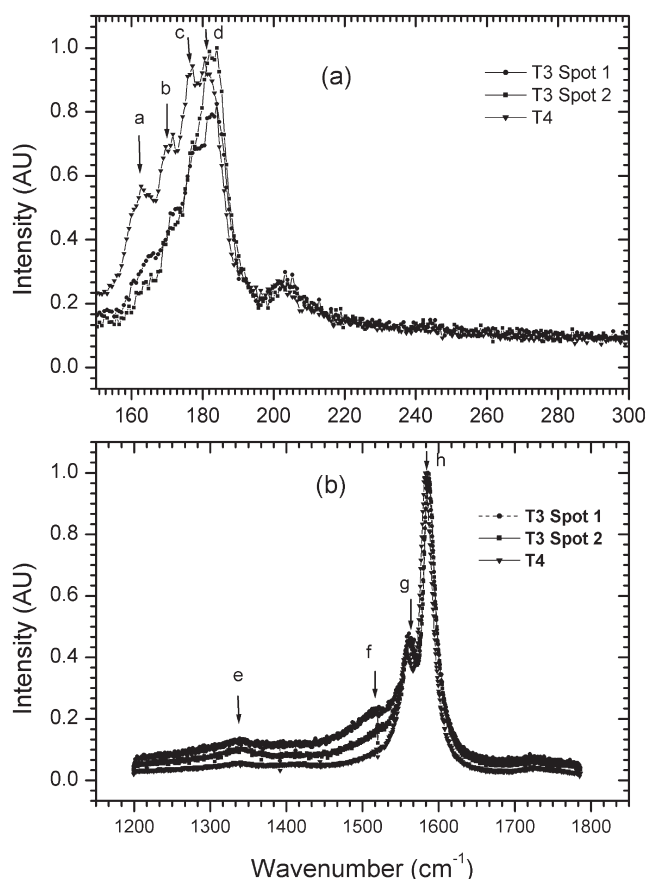


Fig. 9. (a) Effect of adding Fe (top trace, triangles, target T4) as the third catalyst on the RBM frequencies. A shift towards the left of the RBM and a distinct broadening is observed. Clear peaks on the left shoulder are also distinguishable. This points to larger-diameter SWCNTs and a higher abundance at these diameters. (b) The effect of Fe (bottom trace, triangles, target T4) on the D-band and G-bands shows a drop in intensity in the D-band at 1350 cm^{-1} is an indication of reduced disorder in the nanotubes. Reduced intensity on the shoulder at approximately 1525 cm^{-1}

appear to be related to the presence of S and H_2 as such large SWCNTs were not observed in our samples. This was also the view of Iijima *et al.*,²⁵ whose target composition of C:Ni:Co:Fe was similar to but not the same as target T4, which had more than twice the metal concentration for each of Fe, Ni and Co. Several factors ascribed to causing the increase in diameters are listed in ref. 25. The two main factors are the increase in the lattice constant of Fe–Ni–Co complexes and a rise in the aggregation rate of the metal cluster. Further studies are needed to confirm these proposed explanations.

Conclusion

Individual and bundles of single-walled carbon nanotubes were identified in TEM and SEM images. Catalysts were found to be necessary to synthesize the nanotubes. The presence of SWCNTs was verified by Raman spectroscopy. The addition of a third metal catalyst to the target changed the diameter distribution, reduced the defect concentration and also favoured the self-assembly of semiconductor nanotubes. Although limited control

of the nanotubes' diameter was achieved, it is clear that the use and role of multiple catalysts needs further study to achieve the ultimate objective of the controlled synthesis of SWCNTs.

We thank R. Erasmus of the School of Physics and Mike Witcomb of the Microscopy Unit, University of the Witwatersrand, for the Raman spectra and TEM analysis, respectively, and Chris van der Merwe of the Microscopy Unit, University of Pretoria, for the SEM images. We also acknowledge the support of the CSIR National Laser Centre.

- Carbon Nanotechnologies, Inc. Carbon nanotubes – History and development of carbon nanotubes (Buckytubes). Online: <http://www.azonano.com.details.asp?ArticleID=982>.
- Endo M. (1975). *Mecanisme de croissance en phase vapeur de fibres de carbon*. Ph.D. thesis, University of Orleans, Orleans, France.
- Iijima S. (1991). Helical microtubules of graphitic carbon. *Nature* **354**, 56–58.
- Saito R., Fujita M., Dresselhaus G. and Dresselhaus M.S. (1992). Electronic structure of graphene tubules based C_{60} . *Phys. Rev B* **46**, 1804–1811.
- Ajayan P.M., Stephan O., Colliex C. and Trauth D. (1994). Aligned carbon nanotube arrays formed by cutting a polymer resin-nanotube composite. *Science* **265**, 1212–1214.
- Vivien L., Lancon P., Riehl D., Hache F. and Anglaret E. (2002). Carbon nanotubes for optical limiting. *Carbon* **40**(10), 1789–1797.
- Lu J.P. (1997). Elastic properties of carbon nanotubes and nanoropes. *Phys. Rev. Lett.* **79**(7), 1297–1300.
- Harris P.J.F. (1999). *Carbon Nanotubes and Related Structures*. Cambridge University Press, Cambridge.
- Dresselhaus M.S., Dresselhaus G. and Avouris Ph. (eds) (2000). *Carbon Nanotubes: Synthesis, Structure, Properties, and Applications*. Springer-Verlag, Berlin.
- Sinott S.B. and Andrews R. (2001). Carbon nanotubes: synthesis, properties, and applications. *Crit. Rev. Sol. Stat. Mat. Sci.* **26**(3), 145–249.
- Iijima S. (2002). Carbon nanotubes: past, present and future. *Physica B* **323**, 1–5.
- Arepalli S., Holmes W.A., Nikolaev P., Hadjiev V.G. and Scott C.D. (2004). A parametric study of single-wall carbon nanotube growth by laser ablation. *J. Nanosci. Nanotech.* **4**, 762–773.
- Reich S., Li J., Robertson J. (2006). Control the chirality of carbon nanotubes by epitaxial growth. *Chem. Phys. Lett.* **421**, 469–472.
- Rao C.N.R. and Govindaraj A. (2005). *Nanotubes and Nanowires*. RSC Publishing, Cambridge.
- Guo T., Nikolaev P., Rinzler A.G., Tomanek D., Colbert D.T. and Smalley R.E. (1995). Self-assembly of tubular fullerenes. *J. Phys. Chem.* **99**, 10694–10697.
- Thess A., Lee R., Nikolaev P., Dai H., Petit P., Robert J., Xu C., Lee Y.H. Kim S.G., Rinzler A.G., Colbert D.T., Scuseria G.E., Tomanek D., Fischer J.E. and Smalley R.E. (1996). Crystalline ropes of metallic carbon nanotubes. *Science* **273**, 483–487.
- Charlier J.C. and Iijima S. (2000). Growth mechanisms of carbon nanotubes. In *Carbon Nanotubes: Synthesis, Structure, Properties, and Applications*, (eds) M.S. Dresselhaus, G. Dresselhaus and Ph. Avouris, pp. 55–80. Springer-Verlag, Berlin.
- Witanachchi S., Miyawa A.M. and Mukherjee P. (2000). Highly ionized carbon plasma generation by dual laser ablation for diamond-like carbon film growth. *Mat. Res. Soc. Symp.* **617**, J3.6–1–J3.6–6.
- Arepalli S., Nikolaev P. Holmes W. and Scott C.D. (1999). Diagnostics of laser-produced plume under carbon nanotube growth conditions. *Appl. Phys. A* **69**, 1–9.
- Puretzky A.A., Geohagan D.B., Fan X. and Penycook S.J. (2000). Dynamics of single-wall carbon nanotube synthesis by laser vaporization. *Appl. Phys. A* **70**, 153–160.
- Telg H., Maultzsch J., Reich S., Hennrich F. and Thomsen C. (2004). Chirality, distribution and transition energies of carbon nanotubes. *Phys. Rev. Lett.* **93**(17), 177401.1–177404.4.
- Fantini C., Jorio A., Souza M., Strano M.S., Dresselhaus M.S. and Pimenta M.A. (2004). *Phys. Rev. Lett.* **93**(14), 147406.1–147406.4.
- Burghard M. (2005). Electronic and vibrational properties of chemically modified single-wall carbon nanotubes. *Surf. Sci. Rep.* **58**, 1–109.
- Lebedkin S., Schweiss P., Renker B., Malik M., Hennrich F., Neumaier M., Stoermer C., Kappes M.M. (2002). Single-wall carbon nanotubes with diameters approaching 6 nm obtained by laser vaporization. *Carbon* **40**(10), 417–423.
- Zhang M., Yudasaka M. and Iijima S. (2004). Production of large-diameter single-wall carbon nanotubes by adding Fe to a NiCo catalyst in laser ablation. *J. Phys. Chem.* **108**, 12757–12762.

Copyright of South African Journal of Science is the property of South African Assn. for the Advancement of Science and its content may not be copied or emailed to multiple sites or posted to a listserv without the copyright holder's express written permission. However, users may print, download, or email articles for individual use.